Front. Optoelectron.
DOI 10.1007/s12200-015-0483-1

RESEARCH ARTICLE

Highly efficient tunable optical filter based on liquid crystal micro-ring resonator with large free spectral range

Jing DAI[1,2], Minming ZHANG (✉)[1,2], Feiya ZHOU[1,2], Deming LIU[1,2]

1 School of Optical and Electronic Information, Huazhong University of Science and Technology, Wuhan 430074, China
2 Wuhan National Laboratory for Optoelectronics, Huazhong University of Science and Technology, Wuhan 430074, China

Abstract A highly efficient tunable optical filter of liquid crystal (LC) optical micro-ring resonator (MRR) was proposed. The 4-μm-radius ring consists of a silicon-on-insulator (SOI) asymmetric bent slot waveguide with a LC cladding. The geometry of the slot waveguide resulted in the strong electro-optic effect of the LC, and therefore induced an increase in effective refractive index by 0.0720 for the quasi-TE mode light in the slot-waveguide. The ultra-wide tuning range (56.0 nm) and large free spectral range (FSR) (~28.0 nm) of the optical filters enabled wavelength reconfigurable multiplexing devices with a drive voltage of only 5 V. The influences of parameters, such as the slot width, total width of Si rails and slot shift on the device's performance, were analyzed and the optimal design was given. Moreover, the influence of fabrication tolerances and the loss of device were both investigated. Compared with state-of-the-art tunable MRRs, the proposed electrically tunable micro-ring resonator owns the excellent features of wider tuning ranges, larger FSRs and ultralow voltages.

Keywords integrated optics devices, liquid crystals, micro-ring resonator, slot waveguide, wavelength tuning

1 Introduction

Optical networks are widely used in modern communication systems. The use of various optical devices with good performance such as compact size, high fabrication tolerance, low loss, wide tuning range, etc, is becoming more and more significant. Micro-ring resonators (MRR) are one of the key optical devices designed to filter out a very narrow wavelength band from a broad spectrum. To make use of their high wavelength selectivity, they can be used as high-speed tunable filters, add-drop multiplexers, and modulators. As MRRs integrated with silicon-on-insulator (SOI) technology [1,2], they can be very small, high Q factor, and have low losses. Recently, tunable silicon MRRs with wide tuning range and large free spectral range (FSR) are attractive for applications such as reconfigurable dense-wavelength-division-multiplexing (DWDM) [3], reconfigurable multichannel matrix switch [4] and on-chip waveguide sensor multiplexing [5].

Reported tunable optical filters based on MRR can be produced by using various physical effects, including thermo-optic effect [6], electro-optic effect [7], and free carrier plasma dispersion effect [8]. A 10-μm-diameter SOI-based ring resonator with the FSR of 18 nm and the tunable range of 6.4 nm is demonstrated using thermo-optic effect [9], however they suffer from large power dissipation, thermal crosstalk and low integration. Alternatively, both approaches using electro-optic effect of $LiNbO_3$ [10] and free carrier plasma dispersion effect of Si [11] enable fast modulation, but their tuning ranges are small due to the small effective index change. Another method is to combine strip waveguides with nematic LC cladding [12–14], LC molecules are highly birefringent, and orientation can be electrically controlled by external electric fields. The tuning ranges of 31 and 4.5 nm are demonstrated for strip-waveguide MRRs guiding the TM mode and TE mode, but at the expense of smaller FSRs of 4.27 and 4.0 nm respectively [15], and these conventional LC MRRs usually have big sizes (large radii). Moreover, a rather high drive voltage of 100 V is required, which seriously limits the application of such LC MRRs.

In this work, we proposed a novel concept for electrically tunable liquid crystal micro-ring resonator based on an SOI slot-waveguide. The guided-wave slot structure was first proposed in Ref. [16], and this kind of waveguide is able to concentrate a large fraction of the guide mode into the slot region sandwiched between two

Received September 15, 2014; accepted January 21, 2015

E-mail: mmz@hust.edu.cn

strips, and the guide mode is more sensitive to the materials' index distribution change of the slot region. In our proposed configuration, the slot waveguide geometry consists of two doped Si strips and liquid crystal cladding also sandwiched within slot region, the Si rails are conductive and are connected to metal electrodes through the thin conductive Si slab. Through optimal design [17,18], a set of optimal parameters of the bent slot-waveguide ring of 4-μm-radius is chosen as below: the overall Si waveguide width of 400 nm, the slot width of 100 nm, the slot shift of 60 nm. And a LC slot MRR with an ultra-wide tuning range (~56.0 nm) and a large free spectral range (~28.0 nm) can be achieved, where the drive voltage was only 5 V. In addition, the influences of parameters such as the slot width, the total width of Si rails and the slot shift on the device's performance were analyzed. The influence of fabrication tolerances and the loss of device were both also investigated.

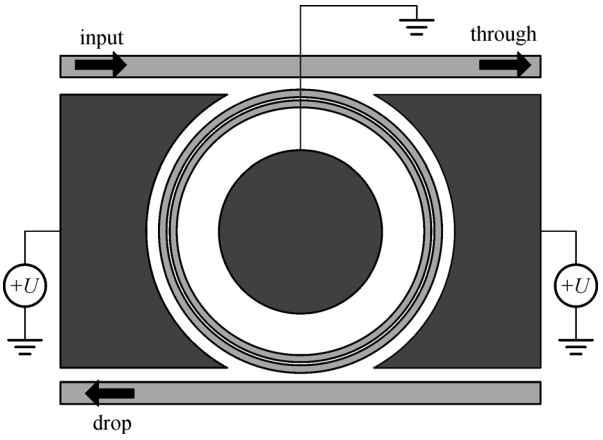

Fig. 1 Schematic top view of the tunable optical filter based on a silicon slot-waveguide micro-resonator infiltrated with LC cladding

2 Device structure and operational principle

Figure 1 shows the schematic diagram of the proposed novel tunable optical filters based on the LC MRR. It relies on the combination of a SOI MRR formed by slot-waveguide with liquid crystal cladding materials. The cross-sectional view of the bend slot-waveguide forming the ring is illustrated in Fig. 2. Some efficient electro-optical devices were realized by employing this kind of SOI strip-loaded slot waveguide [19–21]. In our configuration, the asymmetric ring waveguide is adopted by using two parallel high-index SOI rails with different width, which are spaced by a slot region part. Since the Si slab and rails are assumed as conductors (doped P-type Si), the electrical contact will be generated by putting metal electrodes on top of the strip-loading at a clearance from the waveguide. The external voltage U applied to the metal electrodes induces a strong field within the slot region, as shown in Figs. 1 and 2.

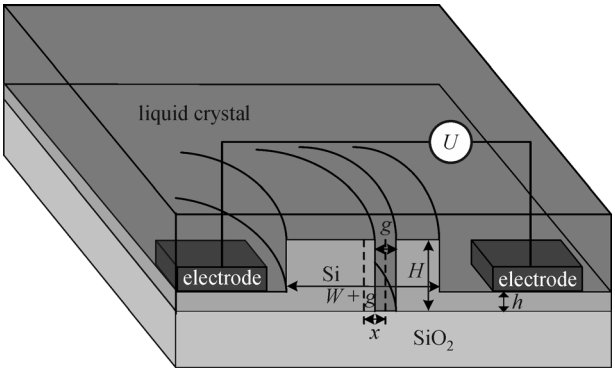

Fig. 2 Schematic cross-sectional view of the SOI strip-loaded bent slot waveguide with LC cladding (where g is the slot width, x represents the slot shift, which is defined as the distance (in nm) from the center of the waveguide to the center of the slot, W ($W = w_l + w_r$) is the total width of two Si rails in the slot waveguide, H and h are the height of the Si rails and Si slab, respectively)

2.1 LC slot waveguide

We use nematic liquid crystal (NLC) as a cladding. It behaves as uniaxial optical properties, where light polarized parallel (perpendicular) to the director experiences the so-called extraordinary (ordinary) refractive index n_e (n_o). The LC's refractive index $n_{LC}(\theta)$ for the quasi-TE optical mode in the slot waveguide can be expressed by [13]

$$n_{LC}(\theta) = \frac{n_o n_e}{\sqrt{n_o^2 \sin^2\theta + n_e^2 \cos^2\theta}}, \quad (1)$$

where θ is defined as the angle between the LC's molecular director and the direction of oscillation of an electric field E (x-direction).

To investigate the electrical and optical characteristics of the LC slot waveguide, we assume two extreme extreme states of the LC slot waveguide as shown in Fig. 3(a), where the slot is centered (non-shift) for the sake of simplicity. First one suggests that without applying a voltage, LC's director field is at a fixed initial state, and LC has a tendency to align to the surface it is attached. Thus, LC molecules align parallel to the waveguide axis [22] (z-direction) as shown in inset (1) of Fig. 3(a). The dominant x-polarized proportion of the quasi-TE optical mode within slot region experiences the ordinary refractive index n_o. Second one suggests that a large voltage is applied, LC molecules will shift in the electric field from the initial state. In particular, the LC molecules within the slot region

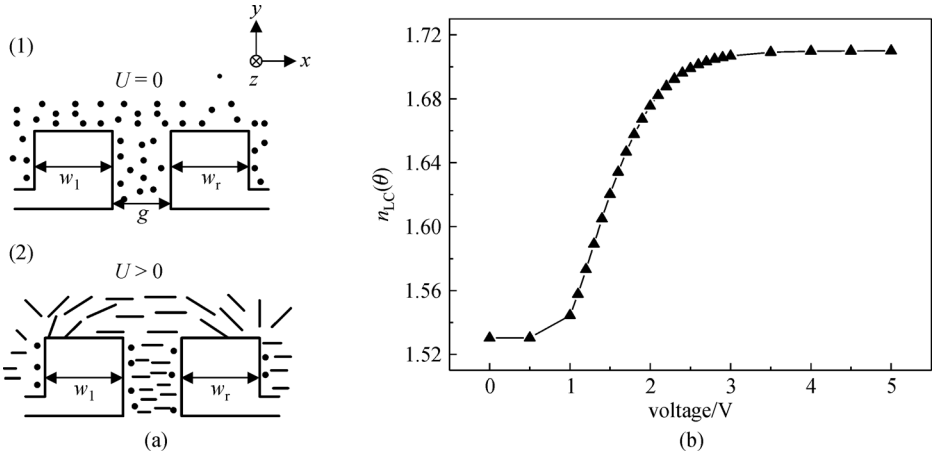

Fig. 3 (a) Two states of LC molecules director for slot waveguides: (1, $U = 0$) no external voltage is applied to the slot waveguide, the LC molecules align parallel to z-direction; (2, $U > 0$) a large external voltage is applied to the slot waveguide, the LC will partly realign along the x-direction; (b) calculated refractive index $n_{LC}(\theta)$ on the voltage for the SOI LC slot waveguide (g = 100 nm)

are oriented along horizontal direction (x-direction) as shown in inset (2) of Fig. 3(a). The dominant x-polarized proportion of the quasi-TE optical mode experiences the extraordinary refractive index n_e.

For a given control electric field required to align the LC molecules, the associated operation voltage depends on the gap between the electrodes. Because the gap of strip-loaded slot waveguides can be made very small (100 nm), the operation voltages can hence be kept very low (only up to 5 V) [19].

Figure 3(b) shows the calculated refractive index $n_{LC}(\theta)$ on the voltage for the LC slot waveguide, where slot width g = 100 nm. The orientation distributions of the NLC molecules at different voltages are calculated by using the finite element method to minimize the Oseen-Frank energy [23]. And the adopted nematic phase liquid crystal is CB5. For the room temperature, the extraordinary (ordinary) refractive indices of the CB5 NLC are shown below: $n_{o,CB5}$ = 1.53, $n_{e,CB5}$ = 1.71 and $\Delta n_{CB5} = n_{e,CB5} - n_{o,CB5}$ = 0.18.

2.2 Wavelength tuning characteristic of the slot micro-ring resonator with LC cladding

The resonance wavelength of a typical MRR is given by [12],

$$\lambda_m = \frac{2\pi R \cdot n_{\text{eff}}}{m}, \tag{2}$$

where n_{eff} is the guide mode's effective refractive index of waveguide, m is an integer, λ_m is the wavelength of the mth resonator mode, R is the radius of resonator (measured from the center of slot waveguide to midpoint of ring).

When a control voltage U is applied to the metal electrodes, a strong electric field will be induced within the slot region. By changing the orientation of the LC molecules with respect to the dominant electric field (E-x) component in the waveguide, we can vary the guide mode's effective refractive index n_{eff} at the slot waveguide, and hence tune the resonance wavelength λ_m of the device.

In this paper, the optical mode characteristics of the SOI slot-waveguide with LC cladding and the refractive index of the guided mode were calculated by the full-vectorial mode solver considering the full anisotropy of nematic LC material [24]. Some numerical simulations were performed with a commercial mode solution software package from Lumerical. To make it clear, some basic parameters were defined. The heights of the Si rails and Si slab are H = 220 nm and h = 60 nm, respectively. The refractive indices of doped Si and lower cladding SiO_2 are 3.48 and 1.46, respectively.

For tunable liquid crystal microring resonator, there are two key performance characteristics that we are concerning: the wavelength tuning range and free spectral range.

To characterize the tuning efficiency by switching the LC director orientation, the tuning range of resonance wavelength can be defined as [14]

$$\Delta\lambda_{\text{Res}} = \frac{\lambda_m \cdot \Delta n_{\text{eff}}}{n_{\text{eff}}}, \tag{3}$$

which describes the dynamic tuning range and Δn_{eff} is the corresponding maximum change value of the effective refractive index.

Another important characteristic for this proposed LC MRR based on a slot-waveguide is the free spectral range (FSR), which can be denoted as below:

$$\Delta\lambda_{\text{FSR}} = \frac{\lambda^2}{2\pi R \cdot n_g}, \tag{4}$$

where n_g is the group index of the slot waveguide.

3 Results and discussion

3.1 LC microring resonator based on the slot and strip waveguide

Compared with the conventional tunable liquid crystal MRR based on strip waveguide, the performance characteristic of LC slot MRR is analyzed. Figure 4 shows that *E*-field amplitude of the optical mode field for slot- and strip- waveguide with LC cladding. TE and TM mode are both taken into consideration for strip-waveguide.

Figure 5 shows that the relationship between the resonant wavelength and the voltage for the quasi-TE mode in our proposed LC MRR, and for the TE and TM mode in the conventional LC MRR as comparisons. A set of optimal parameters of the strip-loaded bend slot-waveguide is specified as below: the radius R = 4 μm, the overall Si waveguide width W = 400 nm, the slot width g = 100 nm, the slot shift x = 60 nm. The optimal design is discussed in Section 3.2. The results illustrate a large resonant wavelength shift of 56.2 nm for our LC MRR, at the same time, the tuning ranges are 31 and 4.5 nm for strip-waveguide MRRs guiding the TM mode and TE mode, respectively. Thus, the dynamic tuning range of resonance wavelength can be enhanced using the slot-waveguide. The significant difference lies to the maximum change value of the effective refractive index. It is easily calculated that, for the LC slot waveguide, Δn_{eff} can reach to about 0.0720. However, for typical strip waveguide with LC cladding, W = 450 nm, h = 220 nm, Δn_{eff} is calculated to be 0.0113 for TE mode and 0.0663 for TM mode by the same numerical method.

From Eq. (4), the corresponding FSR of the proposed LC slot-MRR is calculated to $\Delta\lambda_{\text{FSR}}$ = 28.0 nm. It is larger than that of conventional LC MRRs. And it has seven and eight times the FSRs of 4.27 nm for TM and 4.0 nm for TE mode [15], respectively.

In addition, Fig. 5 shows that another key merit for the slot waveguide-based ring resonator is that the maximum operation voltage only requires 5 V, while it is 100 V for the conventional strip-waveguide. It is because this slot gap can be fabricated with a very small size (in 100 nm) for slot waveguide, whereas all other configurations [12–15] must have electrode separations of at least a few microns,

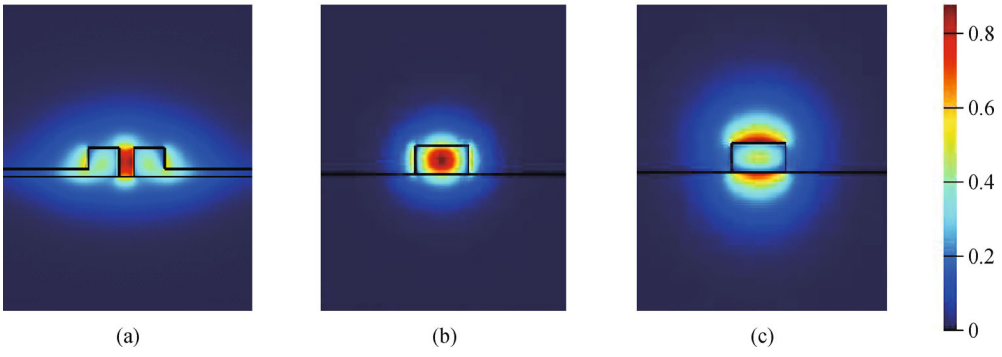

Fig. 4 Comparison of different SOI slot- and strip-waveguides with LC cladding. (a) Transverse *E*-field amplitude of the quasi-TE optical mode field for slot waveguide; (b) transverse *E*-field amplitude of the TE_0 optical mode for strip waveguide; (c) vertical *E*-field amplitude of the TM_0 optical mode for strip waveguide

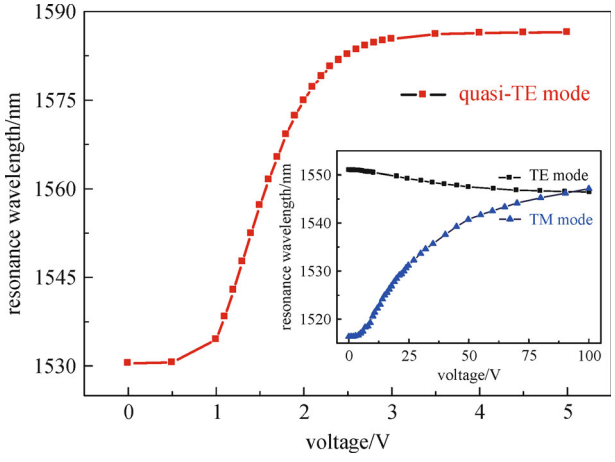

Fig. 5 Relationship between the resonant wavelength and the voltage: for SOI slot LC micro-ring resonator with quasi-TE mode (red curve); for LC MRR based on strip waveguide with TE mode (black curve) and TM mode (blue curve) [9]

by applying the voltage between an indium-tin-oxide (ITO) top electrode and the substrate as bottom electrodes.

3.2 Optical design and analysis of liquid crystal micro-ring resonator

In this section, the influences of parameters including slot width, total width of Si rails and slot shifts on the performance of the micro-ring resonator with small radius (R = 4 μm) will be investigated in detail.

Referring to Eq. (4), it is obviously shown that small radii lead to large FSRs of MRR, the FSR is calculated 28.0 nm when R = 4 μm. In addition, the tuning range drops down when the radii of MRRs decrease. This is because the light in the slot is greatly diminished when traveling around a sharp bend, then the overlap of the optical mode and the LC cladding is diminished. Therefore, the bending effect of waveguide has an important role on the performance characteristics of this device such as the dynamic tuning range of wavelength and FSR. In the following section, we concentrate on the design and analysis of slot-waveguide micro-ring resonator with small radius (R = 4 μm).

Figure 6 shows the tuning range of resonance wavelength calculated as a function of g. Slot width g varies from 40 to 200 nm at a step of 20 nm, at W = 400, 480 and 600 nm ($w_l = w_r$ is fixed at either 200, 240, 300 nm), no slot shift x = 0 nm. It can be seen that, with the increase of g, the tuning range increases at the beginning and reaches to the maximum value. Then after that it drops down. In principle, when the slot waveguide is designed with an optimal wide slot gap, the majority of the modal light lies within the slot sandwiched between two high-index rails. However, the light intensity inside the slot decreases with the increase of the slot width. Therefore, the proportion of the light inside the slot to the overall light in the slot-waveguide reduces. To make a tradeoff between the output wavelength tuning range and the LC molecules infiltrating fabrication, we could not choose too small slot width (the slot is usually at around 100 nm), because the LC molecules should be easily infiltrated into the slot area.

In addition, the tuning range is relatively large at smaller W while the tuning range is relatively small at larger W. The slot waveguide of LC MRR using a very narrow silicon rail is able to obtain large tuning range due to a large evanescent field in the LC cladding of slot. However, the surface roughness significantly increases the waveguide loss. Thus the waveguide width in a slot-waveguide needs to be sufficiently wide to avoid large surface roughness scattering loss.

Next, the tuning range of resonance wavelength $\Delta\lambda_{Res}$ and FSR $\Delta\lambda_{FSR}$ of Si slot-waveguide LC MRR with the change of slot shift are investigated. The light in the slot is greatly diminished when traveling around a sharp bend. Thus, for a bending (especially sharp bend) slot waveguide, we could shift the slot position toward the outside of the bend to maintain the tuning efficiency. This is because shifting the slot ensures that the slot is placed at the region, where the maximum overlap between the two evanescent tails of the high index waveguide modes [17].

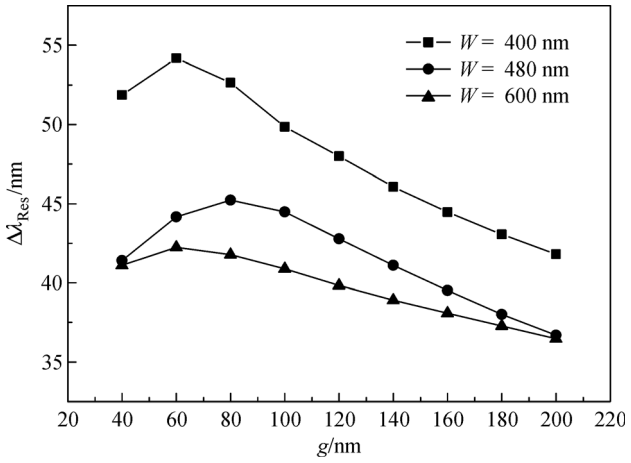

Fig. 6 Tuning range of a silicon single-slot waveguide LC microring (R = 4 μm, non-shift) as a function of the slot width g at different over widths W = 400, 480 and 600 nm

Figure 7(a) shows the tuning range of the resonance wavelength as a function of the slot shifts x at different overall Si rail widths with the following fixed parameters: g = 100 nm, W = 400, 480, 600 nm, and R = 4 μm. It can be seen that the tuning range is maximized at different x for different overall Si rail widths. For example, the maximum of $\Delta\lambda_{Res}$ occurs at $x \approx 60$ nm, $x \approx 40$ nm and $x \approx 40$ nm for W = 400, 480 and 600 nm, respectively. Appropriate slot shift x is then chosen according to this figure to achieve the maximum tuning range of wavelength. Figure 7(b) shows the tuning range of resonance wavelength as a function of slot shifts x at different slot gap widths with the following fixed parameters: W = 400 nm, g = 60, 100, 140 nm, and R = 4 μm. It can be seen that the tuning range is maximized at different x for different slot gap widths. The maximum of $\Delta\lambda_{Res}$ occurs at $x \approx 40$ nm, $x \approx 60$ nm and $x \approx 80$ nm for g = 60, 100 and 140 nm, respectively. Similarly, appropriate slot shift x is then chosen according to this figure to achieve the maximum tuning range. The values of tuning range drop tragically when x deviates from the optimal slot shift. Therefore, the tuning range of the proposed LC micro-ring is very sensitive to the slot shift.

Figures 8(a) and 8(b) show the corresponding FSRs as a function of the slot shift x at different overall Si rail widths W or different slot widths g. From the results, the above FSRs are in range from 24 to 30 nm, and the maximum value is at the corresponding slot shift. The slot shift has little influence on the FSRs of the proposed LC micro-ring.

In a word, considering the influences of parameters including slot width, total width of Si rails and slot shifts, we could choose a set of optimal parameters: the overall Si waveguide width W = 400 nm, slot width g = 100 nm, and slot shift x = 60 nm.

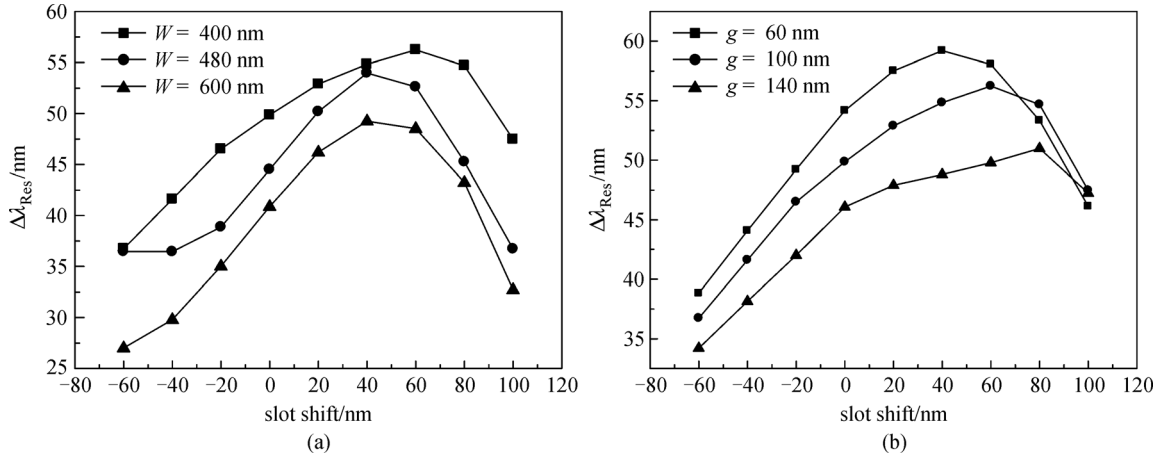

Fig. 7 Tuning range of resonance wavelength of a silicon single-slot waveguide LC micro-ring (R = 4 μm) as a function of the slot shift x (a) at different overall Si rail widths W = 400, 480 and 600 nm with g = 100 nm; and (b) at different slot widths g = 60, 100 and140 nm with W = 400 nm

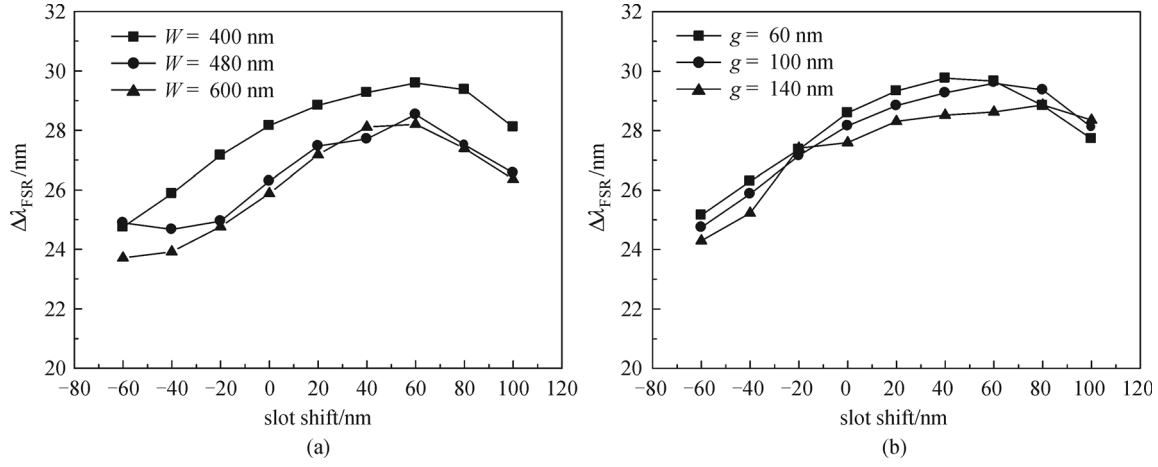

Fig. 8 Free spectrum range of a silicon single-slot waveguide LC micro-ring (R = 4 μm) as a function of the slot shift x (a) at different overall Si rail widths W = 400, 480 and 600 nm with g = 100 nm; and (b) at different slot widths g = 60, 100 and 140 nm with W = 400 nm

3.3 Fabrication tolerances and loss analysis

We further study the fabrication deviation tolerances of the device. For the 4-μm-radius LC slot MRR, assuming the slot with is fixed at 100 nm for g and the slot position x = 60 nm. The dynamic tuning range of the LC slot MRRs is calculated as a function of total Si strips width. From Fig. 9(a), in general, it has a wavelength tuning range above 45 nm throughout a wider range of W (from 300 to 500 nm), and the optimal value of W is equal to 400 nm.

Moreover, slot waveguide fabrication also induces silicon deep etching [25] that could produce non vertical side-walls in the structure. The wavelength tuning ranges are also significantly influenced by this kind of fabrication tolerance. Thus, non vertical sidewall effect on the dynamic tuning range of the slot-waveguide LC MRRs has been investigated in Fig. 9(b). A small decrease of wavelength tuning range on tilting angle θ has been observed.

Concerning the total optical loss of the devices, there are two major sources that contribute to the propagation losses of the slot ring: bending radiation losses due to the bent slot waveguide and additional material losses due to the deposition of the LC cladding. Displacing the slot region from the center of the waveguide toward the outside not only maximizes the power inside the slot, but also reduces the bending losses in the slot waveguide. This is due to the increased confinement in the slot. Figure 10 has shown the electric intensity $|E|^2$ of the quasi-TE optical mode field for the bent asymmetric LC slot-waveguide, the major part of light is confined in the shifting slot. Bending radiation losses could be calculated by monitoring the optical power

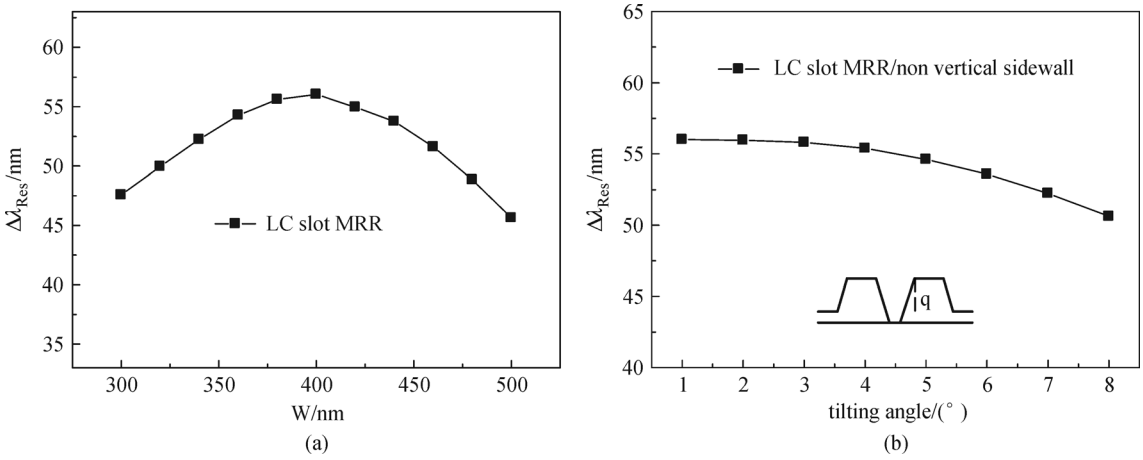

Fig. 9 (a) Tuning range of wavelength as a function of the total Si strips width W (g = 100 nm, R = 4 μm and x = 60 nm); (b) wavelength tuning range for a slot microrings as a function of non vertical sidewall tilting angle θ (W = 400 nm, g = 100 nm, R = 4 μm and x = 60 nm)

of the quasi-TE mode in the bent slot waveguide as a function of the propagation distance, resulting radiation losses of 4.54 dB/mm. The deposition of the LC cladding led to an additional loss of below 2 dB/mm by using special materials with low infrared absorption such as CB5 or E7 [26].

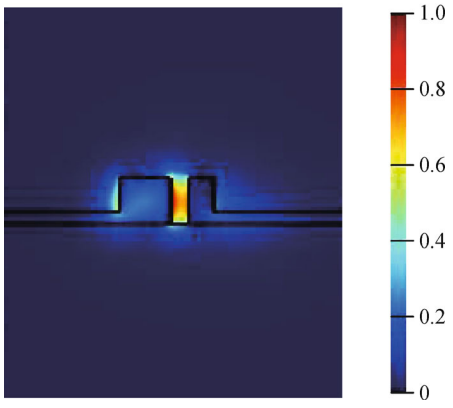

Fig. 10 Electric intensity $|E|^2$ of the quasi-TE optical mode field for the bent LC slot-waveguide with slot shift position x = 60 nm (R = 4 μm, W = 400 nm and g = 100 nm)

4 Conclusions

This paper presented a novel tunable optical filter of microring resonator with wide tuning range large free spectral range and low operation voltage by realigning NLC molecules. By applying a control voltage on the electrodes connected to the thin conductive Si slab, a strong electric field will be induced within the slot region, and it will change the orientation of the LC molecules with respect to the dominant electric field (E-x) component in the waveguide, therefore we can tune the guide mode's effective refractive index n_{eff} at the slot waveguide. After the optimal design, a set of optimal parameters of the slot micro-ring resonator is specified as below: the radius of 4 μm, the overall Si waveguide width of 400 nm, the slot width of 100 nm, the slot shift of 60 nm. The proposed LC MRR provides the excellent performances of an ultra-broadband tuning range (~56.0 nm) and a large free spectral range (~28.0 nm) and an ultralow operation voltage (~5 V). The fabrication of the proposed LC MRR based on an SOI slot waveguide and the design of the electrode structure can be easily demonstrated. For further research of LC micro-ring resonator based on slot waveguide, we will focus on the device fabrication.

Acknowledgements The authors would like to thank Shuchang Yao and Yong Mei for useful discussion. This work was supported by the National High Technology Research and Development Program of China (No. SS2015AA010104), the Major Project of Science and Technology Innovation Program of Hubei Province of China (No. 2014AAA006), and the National Natural Science Foundation of China (Grant No. 61107051).

References

1. Selvaraja S K, Jaenen P, Bogaerts W, Van Thourhout D, Dumon P, Baets R. Fabrication of photonic wire and crystal circuits in silicon-on-insulator using 193-nm optical lithography. Journal of Lightwave Technology, 2009, 27(18): 4076–4083
2. Dumon P, Bogaerts W, Wiaux V, Wouters J, Beckx S, Van Campenhout J, Taillaert D, Luysaert B, Bienstman P, Van Thourhout D, Baets R. Low-loss SOI photonic wires and ring resonators fabricated with deep UV lithography. IEEE Photonics Technology Letters, 2004, 16(5): 1328–1330
3. Basch E B, Egorov R, Gringeri S, Elby S. Architectural tradeoffs for reconfigurable dense wavelength-division multiplexing systems. IEEE Journal of Selected Topics in Quantum Electronics, 2006, 12 (4): 615–626
4. Ng H, Wang M R, Li D, Wang X, Martinez J, Panepucci R R, Pathak

K. 1×4 wavelength reconfigurable photonic switch using thermally tuned microring resonators fabricated on silicon substrate. IEEE Photonics Technology Letters, 2007, 19(9): 704–706
5. Yalcin A, Popat K C, Aldridge J C, Desai T A, Hryniewicz J, Chbouki N, Little B E, King O, Van V, Chu S, Gill D, Anthes-Washburn M, Unlu M S, Goldberg B B. Optical sensing of biomolecules using microring resonators. IEEE Journal of Selected Topics in Quantum Electronics, 2006, 12(1): 148–155
6. Dong P, Qian W, Liang H, Shafiiha R, Feng N, Feng D, Zheng X, Krishnamoorthy A V, Asghari M. Low power and compact reconfigurable multiplexing devices based on silicon microring resonators. Optics Express, 2010, 18(10): 9852–9858
7. Guarino A, Poberaj G, Rezzonico D, Degl'innocenti R, Günter P. Electro-optically tunable microring resonators in lithium niobate. Nature Photonics, 2007, 1(7): 407–410
8. Liu A, Liao L, Rubin D, Nguyen H, Ciftcioglu B, Chetrit Y, Izhaky N, Paniccia M. High-speed optical modulation based on carrier depletion in a silicon waveguide. Optics Express, 2007, 15(2): 660–668
9. Dong P, Qian W, Liang H, Shafiiha R, Feng D, Li G, Cunningham J E, Krishnamoorthy A V, Asghari M. Thermally tunable silicon racetrack resonators with ultralow tuning power. Optics Express, 2010, 18(19): 20298–20304
10. Nishihara H, Haruna M, Suhara T. Optical Integrated Circuit. New York: McGraw-Hill 1985, 36–44
11. Soref R A, Bennett B R. Electrooptical effects in silicon. IEEE Journal of Quantum Electronics, 1987, 23(1): 123–129
12. Maune B, Lawson R, Gunn C, Scherer A, Dalton L. Electrically tunable ring resonators incorporating nematic liquid crystals as cladding layers. Applied Physics Letters, 2003, 83(23): 4689–4691
13. Falco A D, Assanto G. Tunable wavelength-selective add–drop in liquid crystals on a silicon microresonator. Optics Communications, 2007, 279(1): 210–213
14. De Cort W, Beeckman J, James R, Fernandez F A, Baets R, Neyts K. Tuning silicon-on-insulator ring resonators with in-plane switching liquid crystals. Journal of the Optical Society of America B, Optical Physics, 2011, 28(1): 79–85
15. De Cort W, Beeckman J, Claes T, Neyts K, Baets R. Wide tuning of silicon-on-insulator ring resonators with a liquid crystal cladding. Optics Letters, 2011, 36(19): 3876–3878
16. Almeida V R, Xu Q, Barrios C A, Lipson M. Guiding and confining light in void nanostructure. Optics Letters, 2004, 29(11): 1209–1211
17. Anderson P A, Schmidt B S, Lipson M. High confinement in silicon slot waveguides with sharp bends. Optics Express, 2006, 14(20): 9197–9202
18. Kargar A, Chao C. Design and optimization of waveguide sensitivity in slot microring sensors. Journal of the Optical Society of America A, Optics, Image Science, and Vision, 2011, 28(4): 596–603
19. Pfeifle J, Alloatti L, Freude W, Leuthold J, Koos C. Silicon-organic hybrid phase shifter based on a slot waveguide with a liquid-crystal cladding. Optics Express, 2012, 20(14): 15359–15376
20. Barrios C A, Lipson M. Electrically driven silicon resonant light emitting device based on slot-waveguide. Optics Express, 2005, 13 (25): 10092–10101
21. Gould M, Baehr-Jones T, Ding R, Huang S, Luo J, Jen A K, Fedeli J M, Fournier M, Hochberg M. Silicon-polymer hybrid slot waveguide ring-resonator modulator. Optics Express, 2011, 19(5): 3952–3961
22. Desmet H, Neyts K, Baets R. Liquid crystal orientation on patterns etched in silicon on insulator. Integrated Optics, Silicon Photonics, and Photonic Integrated Circuits, 2006, 6183: 61831Z
23. Ge Z, Wu T X, Lu R, Zhu X, Hong Q, Wu S. Comprehensive three-dimensional dynamic modeling of liquid crystal devices using finite element method. Journal of Display Technology, 2005, 1(2): 194–206
24. Fallahkhair A B, Li K S, Murphy T E. Vector finite difference modesolver for anisotropic dielectric waveguides. Journal of Lightwave Technology, 2008, 26(11): 1423–1431
25. Dell'Olio F, Passaro V M. Optical sensing by optimized silicon slot waveguides. Optics Express, 2007, 15(8): 4977–4993
26. Donisi D, Bellini B, Beccherelli R, Asquini R, Gilardi G, Trotta M, d' Alessandro A. A switchable liquid-crystal optical channel waveguide on silicon. IEEE Journal of Quantum Electronics, 2010, 46(5): 762–768

Jing Dai received the B.S. degree in applied physics from the School of Physics of Huazhong University of Science and Technology, Wuhan, China, in 2010. He is currently a Ph.D. candidate in optical engineering from the School of Optical and Electronic of Huazhong University of Science and Technology. His current research interests include silicon-based photonic integrated circuits for optical communications, optical interconnections, and optical sensing.

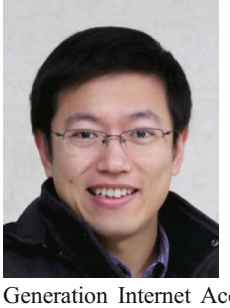

Minming Zhang received the B.S., M.S., and Ph.D. degrees in electronic science and technology from Huazhong University of Science and Technology, Wuhan, China, in 1998, 2001, and 2007, respectively. He is currently an instructor in the same school and a researcher of Wuhan National Laboratory for Optoelectronics and National Engineering Laboratory for Next Generation Internet Access System. His research interests include fiber-optic communications, optical networks, and wireless network.

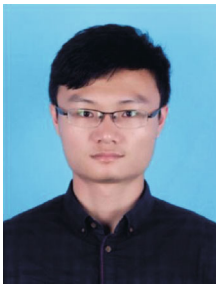

Feiya Zhou received the degree of bachelor in engineering sciences with major in optoelectronics from Huazhong University of Science and Technology (HUST), Wuhan, China, in 2012. He is currently working towards the Ph.D. degree at the School of Optics and Electronic Information, HUST. His current research activities are focused on the nonlinear optical process of silicon devices and the modeling of optical frequency comb in Kerr nonlinear microresonator.

Deming Liu received the M.S. degree from University of Electronic Science and Technology of China and Ph.D. degree from Huazhong University of Science and Technology in China in 1984 and 1999, respectively. He conducted research into the broadband access network at Nanyang Technological University in Singapore as a visiting researcher from 1999 to 2000. He is now a professor and serving as a Director of the National Engineering Laboratory for Next Generation Internet Access System. His research interests include fiber-optic communications, optical networks, and optical sensing.